



Spectrum of imbalanced Alfvénic turbulence at ion-kinetic scales in the solar wind

G. Gogoberidze¹ · Y.M. Voitenko²

Received: 1 April 2020 / Accepted: 3 September 2020 / Published online: 9 September 2020
© Springer Nature B.V. 2020

Abstract Using a semi-phenomenological model of the imbalanced Alfvénic turbulence, we study the turbulence transition from magnetohydrodynamic to sub-ion kinetic scales in the conditions typical for the fast solar wind. We show that the transition takes place in a wide wave number interval where the energy spectrum does not follow any power law. For larger turbulence imbalances, both boundaries of the transition wave number interval shift to larger scales. The energy exchange between dominant and subdominant components of the turbulence is essential in the model reducing the imbalance at kinetic scales; however, the total balance is never reached. Our results are compatible with recent solar wind observations at ion scales and numerical simulations of imbalanced turbulence.

Keywords Sun: solar wind · Turbulence

1 Introduction

The solar wind is the continuous outflow of ionized gas from the solar corona. It is composed primarily of electrons and protons. Alpha particles comprise a few percent of the total and there are traces of heavier ions (Bruno and Carbone 2013). The solar wind flow patterns vary with solar cycle. The most well-organized patterns occur during times of minimum solar activity when there are regions of

steady fast wind that originate from regions of open magnetic field lines where the corona is cooler than in surrounding loops. Fast solar wind has speeds exceeding 600 km/s. The slow solar wind, which is rather unsteady, has speeds less than 500 km/s and originates near closed loops and coronal streamers.

One of the first observations of the solar wind showed that plasma in the wind is turbulent and large scale perturbations are dominated by Alfvén waves propagating outward from the sun (Belcher and Davis 1971). The energy cascade in the Alfvénic turbulence results from nonlinear interactions among counter-propagating waves (Iroshnikov 1963; Kraichnan 1965). According to the Goldreich and Sridhar (1995) theory, in the inertial range the Alfvénic turbulence is dominated by perpendicular cascade. With increasing k_{\perp} the turbulent fluctuations become anisotropic, $k_{\perp} \gg k_{\parallel}$, and the energy spectrum E_k follows Kolmogorov-like scaling $E_k \sim k_{\perp}^{-5/3}$, where k_{\perp} and k_{\parallel} are the perpendicular and parallel wavenumbers with respect to the background magnetic field \mathbf{B}_0 . This kind of scaling is observed in the spacecraft frequency range $10^{-4} - 10^{-1}$ Hz which is interpreted as the inertial interval of the solar wind turbulence (Horbury et al. 2008).

When the perpendicular lengths scale of the perturbations become comparable with the ion gyro-radius ρ_i , Alfvén waves (AWs) transform into kinetic Alfvén waves (Hasegawa and Chen 1976). The properties of kinetic Alfvén waves (KAWs) differ significantly from the magnetohydrodynamic (MHD) AWs. Firstly, KAWs are dispersive and can be strongly affected by wave-particle interactions, e.g., both by proton and electron Landau damping. Secondly, contrary to the MHD AWs, the nonlinear interactions are possible not only among counter-propagating but also among co-propagating KAWs. Kolmogorov-like self-similarity analysis predicts that in the inertial interval of

✉ G. Gogoberidze
grigol_gogoberidze@iliauni.edu.ge

¹ Institute of Theoretical Physics, Ilia State University, 3 ave. Cholokashvili, Tbilisi 0162, Georgia

² 3 Solar-Terrestrial Centre of Excellence, Space Physics Division, Belgian Institute for Space Aeronomy, Ringlaan-3-Avenue Circulaire, 1180 Brussels, Belgium

the KAW turbulence the energy spectrum should scale as $E_k \sim k_{\perp}^{-7/3}$ (Biskamp et al. 1996; Boldyrev et al. 2013).

Recent observations of small-scale magnetic perturbations in the solar wind show that at scales comparable to ρ_i the turbulent spectrum becomes significantly steeper than in the MHD range (see Kiyani et al. (2015) for the recent review) but there is no consensus about exact spectral properties and dominant mechanisms responsible for the observed changes. Leamon et al. (1999) found that at the scales comparable to ρ_i the turbulent spectrum becomes significantly steeper than in the MHD range and the spectral index varies between -2 and -4 . The study of Kiyani et al. (2009) showed that the MHD inertial range is continued by the transition range where no power law is observed and at smaller scales there is another power law dependence with typical spectral index -2.7 . Alexandrova et al. (2009) found that the dispersion range consists of two subintervals, the first one following the power law with the spectral index -2.8 followed by the second one where the energy density is decaying exponentially. According to the analysis of Sahraoui et al. (2010) the dispersion range consists of two power law subintervals. Bruno et al. (2014) found that the spectrum in the dispersion interval is different in the fast and slow solar wind and strongly depends on the cross helicity in the MHD inertial interval. Roberts et al. (2015) analyzed anisotropy of the spectrum using multi-spacecraft observations.

As mentioned above, it is long known that low frequency MHD Alfvénic turbulence in the fast solar wind is strongly imbalanced in the sense that amplitudes of the waves propagating from the sun are significantly larger than amplitudes of sunward propagating waves (Tu et al. 1989). Very recent observations of the high frequency perturbations in the solar wind (Parashar et al. 2018; Bowen et al. 2020) showed that the imbalance presented in the inertial interval weakens but not vanishes at kinetic scales.

Imbalanced MHD turbulence became recently the subject of extensive theoretical and numerical studies. Several phenomenological models have been proposed (Lithwick et al. 2007; Chandran 2008; Beresnyak and Lazarian 2008; Gogoberidze and Voitenko 2016) but no real consensus has been reached to the date. Voitenko and De Keyser (2016) developed a semi-phenomenological model of the imbalanced Alfvénic turbulence covering both the MHD and kinetic range. They found that in the strongly imbalanced case the transition from the MHD to kinetic turbulence occurs through an intermediate interval where the energy transfer is dominated by nonlinear interactions among co-propagating dominant waves. These results were obtained in the assumption that the energy exchange between dominant and subdominant components is negligible and the energy fluxes of these components are conserved. However, both theory (Voitenko 1998) and numerical simulations (Kim and Cho 2015) suggest that there should exist a strong energy exchange between the dominant and subdominant components

of the imbalanced KAW turbulence. Numerical simulations of Cho and Kim (2016) showed that even when the subdominant component was absent initially, it was effectively generated during the typical energy cascade time scale. Similar to the solar wind observations mentioned above Parashar et al. (2018), Bowen et al. (2020) numerical simulations showed that in the imbalanced KAW turbulence imbalance was decreasing with increasing wave number but no equipartition of the energy was reached even at dissipation scales (Kim and Cho 2015).

In the present paper we study the semi-phenomenological model of imbalanced Alfvénic turbulence which covers the MHD and dispersive ranges accounting for the energy exchange between the dominant and subdominant components and compare obtained results with the solar wind observations. The paper is organized as follows: the model is described in Sect. 2, the main results and their comparison with the solar wind observations are presented in Sect. 3, and conclusions are given in Sect. 4.

2 The model of the imbalanced turbulence

Nonlinear dynamic equations for AW amplitudes, which cover both the MHD and dispersive ranges, were derived by Voitenko (1998). Using these nonlinear equations and assuming local interactions, Voitenko and De Keyser (2016) developed the semi-phenomenological turbulence model with the following expression for the nonlinear pumping rates produced by two colliding AWs at wave number k_{\perp} :

$$\gamma_{k_{\pm}}^{NL}(s) = \frac{2+s}{4\pi} k_{\perp} V_A \Delta_{k,s} \frac{B_{k(\pm s)}}{B_0}, \quad (1)$$

where V_A is the Alfvén velocity, $\Delta_{k,s} \equiv \delta V_{ks}/V_A = \sqrt{1 + (k_{\perp} \rho_T)^2} - s$ is the dimensionless phase velocity mismatch of colliding waves, $\rho_T^2 = (3/4 + T_{e\parallel}/T_{i\perp})\rho_i^2$ at $k_{\perp} \rho_i < 1$ and $\rho_T^2 = (1 + T_{e\parallel}/T_{i\perp})\rho_i^2$ at $k_{\perp} \rho_i > 1$, $T_{e\parallel}$ and $T_{i\perp}$ are the parallel electron and perpendicular ion temperatures. Two colliding waves propagating in the same direction (co-collision), produce the nonlinear pumping rate $\gamma_{k_{\pm}}^{NL}(1)$ ($s = 1$ with signs $+$ and $-$ corresponding to the dominant and subdominant components, respectively). Two counter-propagating colliding waves (counter-collision) produce the pumping rate $\gamma_{k_{\pm}}^{NL}(-1)$ ($s = -1$).

In the MHD limit ($k_{\perp} \rho_T = 0$) the velocity mismatch $\Delta_{k,+} = 0$, which makes $\gamma_{k_{\pm}}^{NL}(1) = 0$, i.e. there are no nonlinear interactions produced by co-propagating Alfvén waves. Consequently, there is no energy exchange between the dominant and subdominant components. If we assume that there is no such energy exchange not only in the MHD but also in the dispersive range (Voitenko and De Keyser 2016), then the energy fluxes within both $-$ and $+$ components are constant at all scales and the MHD and kinetic

spectra can be found from the expressions for these fluxes

$$\epsilon_- = \left[\gamma_{k_-}^{NL}(1) + \gamma_{k_-}^{NL}(-1) \right] \frac{B_{k_-}^2}{4\pi}, \quad (2)$$

$$\epsilon_+ = \left[\gamma_{k_+}^{NL}(1) + \gamma_{k_+}^{NL}(-1) \right] \frac{B_{k_+}^2}{4\pi}, \quad (3)$$

in the strong turbulence where the cascade rates are equal to the nonlinear interaction rates, $\gamma_{k_{\pm}}^{TC} \sim \gamma_{k_{\pm}}^{NL}$.

In the MHD range $\gamma_{k_{\pm}}^{NL}(1) = 0$ and, according to Lithwick et al. (2007), the turbulent cascade rate $\gamma_{k_{\pm}}^{TC}(-1) \sim \gamma_{k_{\pm}}^{NL}(-1)$, which results in

$$\frac{\epsilon_+}{\epsilon_-} = \frac{B_{k_+}}{B_{k_-}}. \quad (4)$$

If the turbulence is strongly imbalanced, $\epsilon_+/\epsilon_- \gg 1$, then from (1) it follows that $\gamma_{k_+}^{NL}(1)$ increases with k_{\perp} faster than $\gamma_{k_+}^{NL}(-1)$ and the turbulence cascade eventually arrives to the wave number $k_{\perp*}$,

$$k_{\perp*} \rho_T \approx \sqrt{\frac{\epsilon_-}{\epsilon_+}} \ll 1, \quad (5)$$

where $\gamma_{k_+}^{NL}(1)$ becomes equal to $\gamma_{k_+}^{NL}(-1)$. At larger wave numbers, in the range $\sqrt{\epsilon_-/\epsilon_+} < k_{\perp} \rho_T < 1$, a specific weakly dispersive regime (WDR) of the Alfvénic turbulence should be formed by nonlinear interactions among co-propagating dominant waves. In this range the spectrum is expected to be very steep, $E_{k_+} \sim k_{\perp}^{-3}$ (Voitenko and De Keyser 2016). In the strongly-dispersive regime (SDR), at $k_{\perp} \rho_T \geq 1$, the scaling analysis of equations (2)-(3) predicts the standard spectra $E_{k_{\pm}} \sim k_{\perp}^{-7/3}$ of the strong KAW turbulence.

However, the condition $\sqrt{\epsilon_-/\epsilon_+} = \sqrt{B_{k_+}/B_{k_-}} \ll 1$ is not satisfied even in the most imbalanced quiet fast streams of the solar wind (see, e.g., Wicks et al. (2011), Gogoberidze et al. (2012) and references therein). In this case behavior of the energy spectrum in the transition range between the MHD range and the SDR is not obvious. Moreover, the energy fluxes ϵ_{\pm} are constant only in the MHD limit. In the case of dispersive KAWs co-propagating dominant KAWs can generate subdominant waves, and vice versa (Voitenko (1998), Voitenko and De Keyser (2011), Passot and Sulem (2019) and references therein). Such energy exchange has been observed in electron-MHD numerical simulations of the KAW turbulence in the SDR (Cho and Kim 2016) - even when the subdominant component was initially absent, it was effectively generated by the dominant component during the typical cascade timescale. The semi-phenomenological model of the imbalanced Alfvénic turbulence accounting for the energy exchange between counter-propagating wave fluxes has been developed by Gogoberidze and Voitenko (2020). It was shown that similar to the

equation (1), pumping rate of the dominant component energy to the subdominant component $\gamma_{k_-}^{EX}$ can be modeled as

$$\gamma_{k_-}^{EX} = \frac{1}{4\pi} k_{\perp} V_A \Delta_{k,1} \frac{B_{k_+}^2}{B_{k_-} B_0} = \gamma_{k_+}^{NL}(1) \frac{B_{k_+}}{B_{k_-}}. \quad (6)$$

There is also the process where the subdominant waves transfer part of their energy back to the dominant component. Corresponding pumping rate is given by the following expression

$$\gamma_{k_+}^{EX} = \frac{1}{4\pi} k_{\perp} V_A \Delta_{k,1} \frac{B_{k_-}^2}{B_{k_+} B_0}. \quad (7)$$

To incorporate the energy exchange effects in the phenomenological model we add the corresponding terms to the equations (2)-(3)

$$\epsilon_- + \gamma_{k_-}^{EX} \frac{B_{k_-}^2}{4\pi} - \gamma_{k_+}^{EX} \frac{B_{k_+}^2}{4\pi} = \left[\gamma_{k_-}^{NL}(1) + \gamma_{k_-}^{NL}(-1) \right] \frac{B_{k_-}^2}{4\pi}, \quad (8)$$

$$\epsilon_+ - \gamma_{k_-}^{EX} \frac{B_{k_-}^2}{4\pi} + \gamma_{k_+}^{EX} \frac{B_{k_+}^2}{4\pi} = \left[\gamma_{k_+}^{NL}(1) + \gamma_{k_+}^{NL}(-1) \right] \frac{B_{k_+}^2}{4\pi}. \quad (9)$$

The left hand sides of these equations represent the scale dependent fluxes of counter propagating waves. In the next section we use equations (8)-(9) to study transition of Alfvénic turbulence from the MHD range to the SDR for the level of imbalances typical for the solar wind turbulence.

3 The results

In this section we present solutions of the equations (8)-(9) and compare obtained results with the existing solar wind observations and numerical simulations. The equations (8)-(9) represent the set of algebraic equations and it is solved for various values of k_{\perp} for fixed value of the inertial range flux ratio ϵ_+/ϵ_- . Note that according to equation (4), in the inertial interval the ratio of fluxes equals to the ratio of amplitudes $B_{k_+}/B_{k_-} = \epsilon_+/\epsilon_-$. It is known that even in the quiet fast streams of the solar wind the amplitude ratio of counter propagating Alfvén waves never exceeds one order of magnitude (see, e.g., Wicks et al. (2011), Gogoberidze et al. (2012) and references therein) $B_{k_+}/B_{k_-} = \epsilon_+/\epsilon_- \lesssim 10$. Figure 1 shows the compensated energy spectra $E_{\pm}(k_{\perp}) k_{\perp}^{5/3}$ for the imbalance $\epsilon_+/\epsilon_- = 8$. The solid/dashed lines correspond to the dominant/subdominant components respectively. The dashed-dotted/dotted lines represent solutions of equations (2)-(3), i.e., represent the spectra without the energy exchange effect. As can be seen in Fig. 1, in the transition range

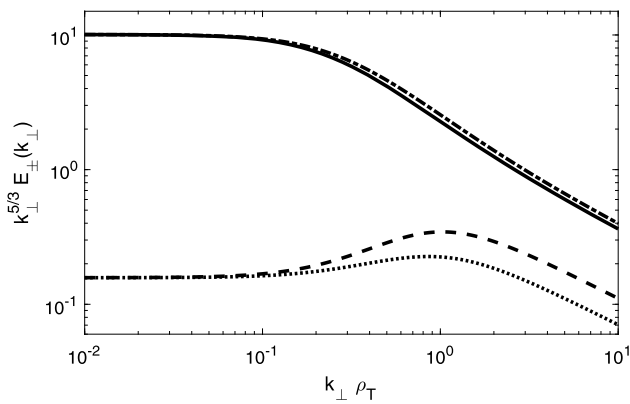


Fig. 1 The compensated energy spectra $E_{\pm}(k_{\perp})k_{\perp}^{5/3}$ for $\epsilon_{+}/\epsilon_{-} = 8$. The solid/dashed lines correspond to the dominant/subdominant components respectively. The dashed-dotted/dotted lines represent the same spectra $E_{\pm}(k_{\perp})k_{\perp}^{5/3}$ without the energy exchange effect

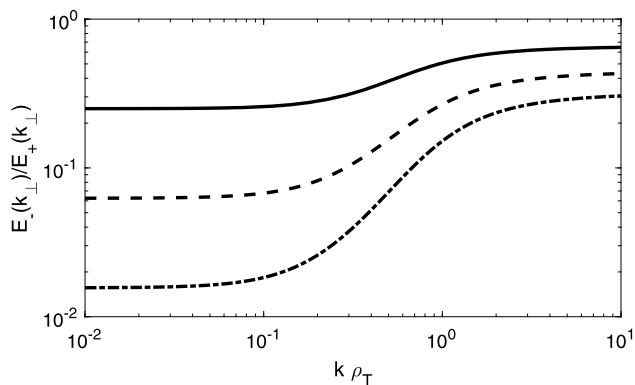


Fig. 2 Dependence of $E_{-}(k_{\perp})/E_{+}(k_{\perp})$ on the normalized wave number $k_{\perp}\rho_T$. Solid, dashed and dashed-dotted lines correspond to $\epsilon_{+}/\epsilon_{-} = 2, 4, 8$, respectively

$0.2 < k_{\perp}\rho_T < 1$ energy exchange causes significant enhancement of $E_{-}(k_{\perp})$ but total equipartition of the energy is not reached. Figure 2 shows dependence of the energy ratio $E_{-}(k_{\perp})/E_{+}(k_{\perp})$ on the normalized wave number $k_{\perp}\rho_T$ for $\epsilon_{+}/\epsilon_{-} = 2, 4, 8$ (solid, dashes, dashed-dotted lines, respectively). The asymptotic values of the ratio $E_{-}(k_{\perp})/E_{+}(k_{\perp})$ for $k_{\perp}\rho_T \gg 1$, are $E_{-}(k_{\perp})/E_{+}(k_{\perp}) = 0.3, 0.42, 0.55$ respectively for $\epsilon_{+}/\epsilon_{-} = 2, 4, 8$.

The results shown in Figs. 1, 2 are in qualitative agreement with the results of both recent solar wind observations (Parashar et al. 2018; Bowen et al. 2020) and the numerical simulations of KAW turbulence (Kim and Cho 2015; Cho and Kim 2016). Analysis of high frequency data from Magnetospheric Multi-scale Mission (Parashar et al. 2018) and Parker Solar Probe (Bowen et al. 2020) showed that the imbalance of turbulence at MHD scales significantly decreases in the transition range but does not vanish at ion-kinetic scales. Numerical simulations of the imbalanced KAW turbulence showed that the imbalance was decreasing with in-

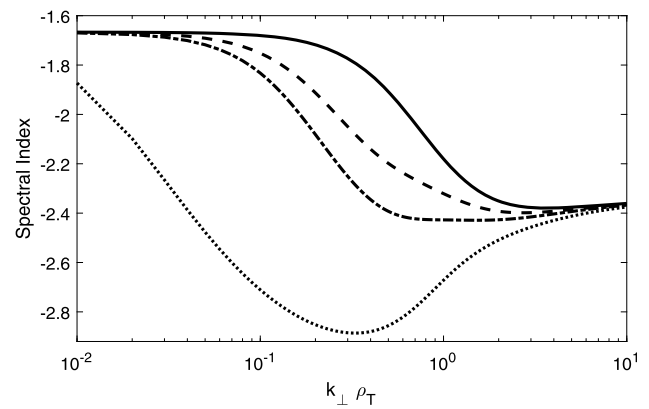


Fig. 3 The local value of the energy spectral index. Solid, dashed, dashed-dotted and dotted lines correspond to $\epsilon_{+}/\epsilon_{-} = 2, 4, 8, 1000$, respectively

creasing wave number but no equipartition of the energy was reached even at dissipation scales (Kim and Cho 2015). Figure 3 shows the local spectral index of the total energy $E_{-}(k_{\perp}) + E_{+}(k_{\perp})$. Solid, dashed, dashed-dotted and dotted lines correspond to the cases $\epsilon_{+}/\epsilon_{-} = 2, 4, 8, 1000$, respectively. First of all, we see that WDR with the spectral index approaching -3 predicted by Voitenko and De Keyser (2016) is indeed possible, but requires extremely large values of $\epsilon_{+}/\epsilon_{-}$ not observed in the solar wind.

For small and moderate imbalances ($\epsilon_{+}/\epsilon_{-} = 2, 4, 8$) Fig. 3 shows that there is a quite wide transition range from MHD to SDR where the spectral slope decreases smoothly and therefore in this range no power law behavior is expected. This fully agrees with the solar wind data analysis of Kiyani et al. (2009, 2015) where no power law was observed in the quite wide transition range from MHD to sub-ion ranges.

The equation (5) shows that beginning of the transition range should shift to larger scales with the increasing imbalance $\epsilon_{+}/\epsilon_{-}$ whereas beginning of SDR is expected at $k_{\perp}\rho_T \approx 1$ regardless of the imbalance level. As seen in Fig. 3, not only the beginning but also the end point of the transition range shifts to the smaller wave numbers with increasing $\epsilon_{+}/\epsilon_{-}$. The fact that the end point of the transition range also moves to the larger scales does not contradict to the equation (5) because physically it is caused by nonlinear interactions of co-propagating waves (which for extremely high imbalances lead to the formation of the WDR). Therefore, for typical solar wind parameters our model predicts shift of the transition range to the larger scales with increasing imbalance and this relation can be tested by means of the modern solar wind data analysis (Parashar et al. 2018; Bowen et al. 2020).

In the SDR our model predicts self-similar KAW turbulence spectrum (Biskamp et al. 1996; Boldyrev et al. 2013) with the spectral index $-7/3$. Steeper spectra frequently observed in the SDR (Lithwick et al. 2007; Kiyani et al. 2009;

Alexandrova et al. 2009) can be caused by the influence of intermittency (Boldyrev et al. 2013) transition from strong to weak turbulent regime (Voitenko and De Keyser 2011) or the linear Landau damping of KAWs. These effects were ignored in the present analysis and will be considered elsewhere.

4 Conclusions

We studied the semi-phenomenological model of the imbalanced Alfvénic turbulence in the solar wind accounting for the energy exchange between counter-propagating wave fluxes in the dispersive range. The model covers the MHD, transition and SDR scales. Our main results are as follows:

- For the moderate imbalances which are typical for the fast solar wind, the transition range between the MHD and SDR is quite wide, with the slowly changing local spectral slope. These results qualitatively agree with the spectral analysis of the solar wind turbulence reported by Kiyani et al. (2009, 2015).
- Our model predicts that both the lower and the upper boundaries of the transition wave number interval depend on the turbulence imbalance and shift to larger scales with larger imbalance. These results can be verified by observations.
- The turbulence imbalance becomes scale-dependent and reduces significantly in the transition range, but the total equipartition is not reached. These results qualitatively agree with the recent solar wind observations at ion scales (Parashar et al. 2018; Bowen et al. 2020) and the numerical simulations of imbalanced KAW turbulence (Kim and Cho 2015; Cho and Kim 2016).

Acknowledgements We are grateful to the anonymous referee for the valuable suggestions. This work has been supported by Shota Rustaveli National Science Foundation grants FR-18-19964.

Publisher's Note Springer Nature remains neutral with regard to jurisdictional claims in published maps and institutional affiliations.

References

- Alexandrova, O., Saur, J., Lacombe, C., Mangeney, A., Mitchell, J., Schwartz, S.J., Robert, P.: *Phys. Rev. Lett.* **103**, 165003 (2009)
- Belcher, J.W., Davis, L.: *J. Geophys. Res.* **76**, 3534 (1971)
- Beresnyak, A., Lazarian, A.: *Astrophys. J.* **682**, 1070 (2008)
- Biskamp, D., Schwarz, E., Drake, J.F.: *Phys. Rev. Lett.* **76**, 1264 (1996)
- Boldyrev, S., Horaites, K., Xia, Q., Perez, J.C.: *Astrophys. J.* **777**, 41 (2013)
- Bowen, T.A., et al.: *Astrophys. J.* **125**, 025102 (2020)
- Bruno, R., Carbone, V.: *Living Rev. Sol. Phys.* **10**, 2 (2013)
- Bruno, R., Trenchi, L., Telloni, D.: *Astrophys. J. Lett.* **793**, L15 (2014)
- Chandran, B.D.G.: *Astrophys. J.* **685**, 646 (2008)
- Cho, J., Kim, H.: *J. Geophys. Res.* **121**, 6157 (2016)
- Gogoberidze, G., Voitenko, Y.M.: *Astrophys. Space Sci.* **361**, 364 (2016)
- Gogoberidze, G., Voitenko, Y.M.: *Mon. Not. R. Astron. Soc.* **497**, 3472 (2020)
- Gogoberidze, G., Chapman, S.C., Hnat, B., Dunlop, M.: *Mon. Not. R. Astron. Soc.* **426**, 951 (2012)
- Goldreich, P., Sridhar, S.: *Astrophys. J.* **438**, 763 (1995)
- Hasegawa, A., Chen, L.: *Phys. Fluids* **19**, 1924 (1976)
- Horbury, T.S., Forman, M., Oughton, S.: *Phys. Rev. Lett.* **101**, 175005 (2008)
- Iroshnikov, P.S.: *Astron. Zh.* **40**, 742 (1963)
- Kim, H., Cho, J.: *Astrophys. J.* **801**, 75 (2015)
- Kiyani, K.H., Chapman, S.C., Khotyaintsev, Y.V., Dunlop, M.W., Sahraoui, F.: *Phys. Rev. Lett.* **103**, 075006 (2009)
- Kiyani, K.H., Osman, K.T., Chapman, S.C.: *Philos. Trans. R. Soc. A, Math. Phys. Eng. Sci.* **373**(2041), 20140155 (2015)
- Kraichnan, R.H.: *Phys. Fluids* **8**, 1385 (1965)
- Leamon, R.J., Smith, C.W., Ness, N.F., Wong, H.K.: *J. Geophys. Res.* **104**, 22331 (1999)
- Lithwick, Y., Goldreich, P., Sridhar, S.: *Astrophys. J.* **655**, 269 (2007)
- Parashar, T., et al.: *Phys. Rev. Lett.* **121**, 265101 (2018)
- Passot, T., Sulem, P.L.: *J. Plasma Phys.* **85**, 905850301 (2019)
- Roberts, O.W., Li, X., Jeska, L.: *Astrophys. J.* **802**, 21 (2015)
- Sahraoui, F., Goldstein, M.L., Belmont, G., Canu, P., Rezeau, L.: *Phys. Rev. Lett.* **105**, 131101 (2010)
- Tu, C.-Y., Marsch, E., Thieme, K.M.: *J. Geophys. Res.* **94**, 11739 (1989)
- Voitenko, Y.M.: *J. Plasma Phys.* **60**, 497 (1998)
- Voitenko, Y., De Keyser, J.: *Nonlinear Process. Geophys.* **18**, 587 (2011)
- Voitenko, Y., De Keyser, J.: *Astrophys. J. Lett.* **832**, L20 (2016)
- Wicks, R.T., Horbury, T.S., Chen, C.H.K., Schekochihin, A.A.: *Phys. Rev. Lett.* **106**, 045001 (2011)

Reproduced with permission of copyright owner. Further reproduction prohibited without permission.